Optimization of the effective light attenuation length of YAP:Ce and LYSO:Ce crystals for a novel geometrical PET concept

I. Vilardi, F. Ciocia, N. Colonna, R. De Leo*, L. Lagamba, S. Marrone, E. Nappi, G. Tagliente, A. Valentini
Physics Dept. and INFN Section of Bari, Via Orabona 4, Bari, Italy
A. Braem, E. Chesi, C. Joram, J. Séguinot, P. Weilhammer
CERN PH-Department, CH-1211 Geneva, Switzerland
F. Corsi, A. Dragone
DEE Politecnico di Bari – MICROLABEN s.r.l., Bari, Italy
F. Cusanno, F. Garibaldi
Laboratory of Physics, ISS, Viale Regina Elena 299, Rome, Italy
H. Zaidi
Division of Nuclear Medicine, Geneva University Hospital, CH-1211 Geneva, Switzerland

Abstract—**The effective light attenuation length in thin bars of YAP:Ce and LYSO:Ce crystals has been studied for different coatings of the lateral surfaces of the scintillators. This physical parameter plays a key role in a novel 3D PET concept based on axial arrays of long scintillator bars read out at both ends by Hybrid Photodetectors (HPD). The parameter influences the spatial, energy, and time resolutions of such a device. The expected resolutions let the novel concept appear competitive compared to existing traditional PET devices. In this paper we show that the effective light attenuation length can be tuned to the desired value by wrapping the lateral surfaces of the crystals or by coating them with layers of Cr or Au of different thickness. The studies have been carried out with long YAP and LYSO scintillator bars, read out by standard photomultiplier tubes. Even though the novel PET device is planned to use different scintillators and HPD readout, the results described here prove the feasibility of an important aspect of the concept and explore the potential resolution of the device.**

Keywords: YAP:Ce; LYSO:Ce; molecular imaging; PET; HPD.

I. INTRODUCTION

The CIMA collaboration [1] has recently proposed a novel 3D PET geometrical concept [2] based on axially oriented arrays of long scintillator bars (e.g. 3.2×3.2×100 mm^3), read out at the two ends by Hybrid Photodetectors (HPD) [3]. A schematic view of the novel device is shown in Fig.1. The unambiguous definition of the gamma interaction point in a real 3D geometry eliminates the parallax error due to the unknown depth of interaction (DoI) of the deposited energy [4] thus improving the spatial resolution, sensitivity and contrast of the PET performance in the field of molecular imaging. The concept is new compared to available PETs which are based [2] on radial crystal arrangements and block readout schemes (Anger logic). It is conceptually different from the phoswich technique which also aims to measure the DoI. The 3D Axial PET concept provides higher efficiency, due to the absence of limitations imposed by the detector thickness in the radial direction (see Fig. 1), and to the possibility [4] to recover a fraction of γ's undergoing double scattering (Compton and photoelectric) in the crystal array.

Scintillation light produced in the crystal propagates to the two ends by total internal reflection from the crystal surfaces. On its way part of the light is absorbed with a characteristic attenuation length. While the transverse coordinates (*x, y*) of detected photons are determined from the address (i.e. position) of the hit crystal, $\sigma_{x,y}$ = 3.2/√12 = 0.9 mm, the axial (*z*) coordinate is derived with precision σ_z from the ratio of the photoelectron yield N_1 and N_2 measured at the two ends of the long crystals:

$$z=\frac{1}{2}\left(\lambda_{eff}\ln\frac{N_1}{N_2}+L_C\right);\quad \sigma_z=\frac{\lambda_{eff}}{\sqrt{2N_o}}\left(\exp\frac{z}{\lambda_{eff}}+\exp\frac{L_C-z}{\lambda_{eff}}\right)^{1/2} \qquad (1)$$

with L_C being the length of the crystal, λ_{eff} the effective light attenuation length of the crystals. It is different from the bulk value λ_{bulk} as it takes into account the real path of the photons, which is increased due to the multiple bounces: $\lambda_{eff} \approx 0.8 \cdot \lambda_{bulk}$. N_0 is the number of photoelectrons for $\lambda_{eff} \rightarrow \infty$. Its value depends both on the physical and optical properties of the chosen scintillator (incl. surface coating/wrapping) and the characteristics of the photodetector. It is implicitly assumed that the photoelectron yields N_1 and N_2 depend exponentially on the average path length of the scintillation photons belonging to one gamma ~exp(z/λ_{eff}). The expression for σ_z accounts for the photoelectron statistics, however it ignores the fluctuations of the path lengths w.r.t. the average value. In order to achieve a competitive σ_z the crystal length L_C needs to be limited to values below ~150 mm and λ_{eff} has to be optimized depending on the chosen crystal and its length. The two parameters L_C and λ_{eff} play obviously *a* key role in the proposed geometrical PET concept.

* Corresponding author, e-mail: deleo@ba.infn.it

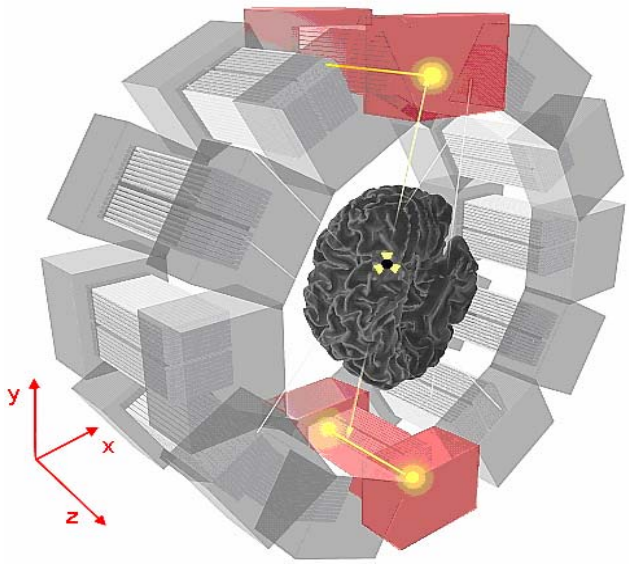

Fig.1. The novel 3D axial PET concept. Matrices of axially displaced long crystals are read out on both sides by HPDs.

In this paper we present an experimental study to optimize the effective crystal light attenuation length, λ_{eff}, for a set of polished YAP:Ce scintillators of dimensions 3.2 x 3.2 x 100 mm^3 produced by Preciosa Crytur Co at Turnov, Czech Republic, and for a few samples of polished LYSO:Ce of equal size, produced by Photonic Materials, Scotland. We have measured the λ_{eff} parameter in polished and wrapped crystals by means of 511 keV γ rays emitted from a ^{22}Na source.

Techniques to modify the reflectivity of the crystal by wrapping, coating or roughing its surface, have been described in the literature (see e.g. Ref. 5). We show here that, by coating the lateral surfaces of the crystals with layers of evaporated Cu or Au of various thicknesses, it is possible to tune λ_{eff} to achieve a value which leads to optimized spatial, energy, and time resolutions.

A simulation with a custom developed photo tracking code [2] has been used to extrapolate the present study to other crystal lengths and to other scintillators, such as $LaBr_3$ and LSO having both high photofraction and light yield, and hence appear more suited for PET devices. Experimental studies with these crystals are in progress.

II. EXPERIMENTAL SETUP AND RESULTS

A. Experimental apparatus

We have carried out the experimental studies with YAP and LYSO crystals of dimensions 3.2 × 3.2 × 100 mm^3. The thickness of the crystal has been chosen to obtain an excellent transverse spatial resolution and are matched to the pixel size of the HPDs that will be used in the final project [2,3]. A set-up has been built (Fig. 2), which allows measuring crystal energy linearity and attenuation lengths. The crystal under test is read out by two photodetectors and is placed on a platform remotely

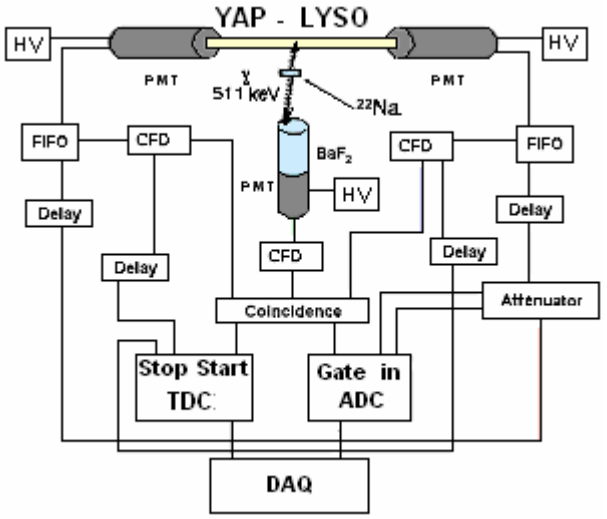

Fig. 2. Schematic setup used to measure effective attenuation lengths. For energy linearity measurements a similar setup has been used with the BaF_2 detector and its associated electronics removed.

movable by a step motor. For the present study H3164-10 PMTs with borosilicate windows have been used as photodetectors, while the HPD of the final project will be equipped with a thin sapphire window. This leads to almost perfect refractive index matching and therefore minimizes transmission losses at the crystal/detector interface.

To measure the effective attenuation lengths, a point-like ^{22}Na source sealed in plastic has been used. One of the two resulting 511 keV γ-rays is detected by the crystal that is placed in coincidence with a BaF_2 detector placed on one side of the linear stage at a fixed position with respect to the γ-source. To measure energy linearity, a similar setup has been used employing various radioactive sources as ^{88}Y, ^{60}Co ^{137}Cs, ^{22}Na, and ^{241}Am. In these measurements, the BaF_2 detector and its associated electronics has been removed. Each radioactive source is encapsulated in a lead shield with a small hole in the center and displaced from the tested YAP or LYSO crystal in order to illuminate a 2 mm wide slide of its lateral surface. Conventional NIM electronics has been used. The data acquisition has been restricted to coincident timing signals from the *crystal-left*, *crystal-right* and BaF_2 PMTs. Timing signals were formed by employing constant fraction discriminators (CFD). A scheme of the electronics used is included in Fig. 2.

B. Energy linearity

Energy spectra for polished YAP and LYSO scintillator exposed to 511 keV γ-ray impinging at the center of the crystal lateral surface are shown in Fig. 3. The shown spectra have been obtained by summing the ADC signals of the left and right crystal PMTs. The positions of the photoelectric peaks in the ADC spectra for this and the other explored sources, plotted in Fig. 4 versus the γ-ray energy, show a very linear behaviour. The non-linearity coefficient, defined as [6]:

$$\sigma_{nl} = \sqrt{\frac{1}{N}\sum_{i=1}^{N}\left(\frac{Q(E_i)}{Q(^{137}Cs)} - \frac{E_i}{661.6}\right)} \qquad (2)$$

and summed over the seven investigated energies results to be: σ_{nl}(YAP) = 0.0125, σ_{nl}(LYSO) = 0.054.
These values are very low compared to those in Ref. 6, even if obtained in a different energy range.

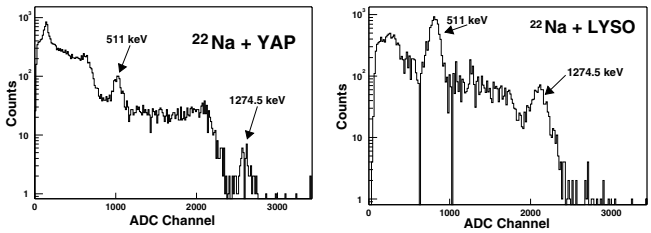

Fig. 3. Energy spectra for polished YAP (left panel) and LYSO (right panel) scintillators exposed to 511 keV γ-ray impinging at the center of the crystal lateral surface. The spectra have been obtained by summing the crystal left and right ADC signals.

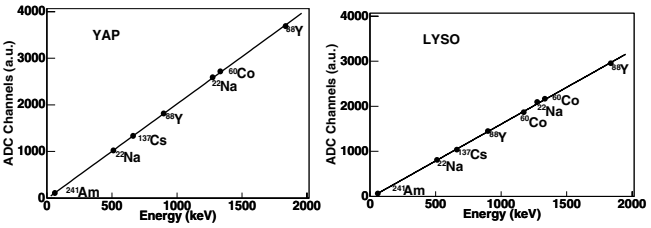

Fig. 4. Energy linearity for YAP (left panel) and LYSO (right panel): the ADC position of the photoelectric peaks for spectra as those in Fig. 3, are plotted versus the γ-ray energy (from 60 keV to 1.8 MeV). The line in each panel represents a linear fit to the data.

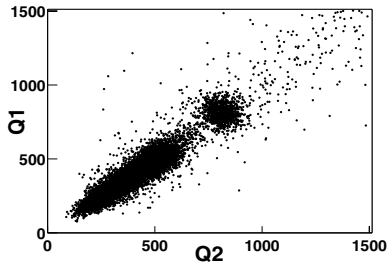

Fig. 5. Bidimensional spectrum (ADC left versus ADC right) for a 3.2x3.2x100 mm^3 polished LYSO crystal exposed to 511 keV γ-rays at the center (z=5 cm) of its lateral.

C. *Measurement of the effective light attenuation length λ_{eff}*

The signal amplitudes measured at left and right ends of the crystal bar, are highly correlated. Fig. 5 illustrates this for a polished YAP scintillator exposed to 511 keV γ-rays impinging in the middle (z=5 cm) of the crystal bar. The central spot in the figure corresponds to the photopeak. In Fig. 6 we plot he charge Q of the photopeak as obtained from the left ADC spectrum scanning polished YAP and LYSO crystals in the z-range from 1 to 9 cm, in steps of 1 cm. The linear

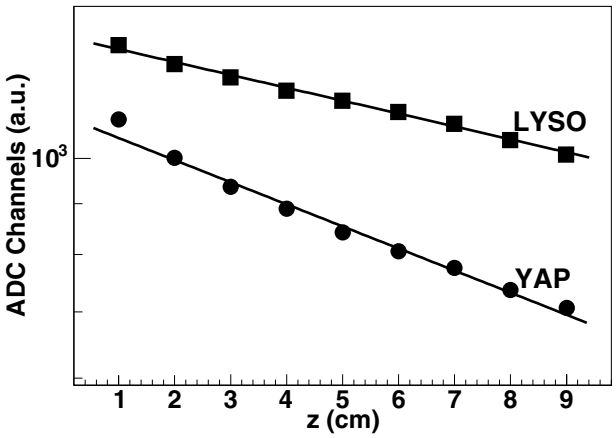

Fig. 6. The signal amplitude (log scale) measured at one end of the bar (here left) versus the z-position of the 511 keV photons for a polished YAP and LYSO crystal. The analysis is based on the photopeak only.

behaviour in log scale means that one exponential ($Q_o \cdot exp(-z/\lambda_{eff})$) is sufficient to reproduce the PMTs pulse heights measured by moving the source along the crystal length.

The average effective attenuation length evaluated on a set of sixteen polished YAP crystals results to be λ_{eff} = 20.8±0.8 cm. This value is higher than that reported in the literature [2] and, as we discuss below, would lead to a reduced resolution of our z-reconstruction method. For a set of three polished LYSO crystals an even higher value, λ_{eff} = 42±0.6 cm, has been obtained.

In Fig. 7 we summarize the results of the same z-scans with YAP crystal bars where the lateral surfaces have been coated or wrapped. The experimental data show that also the behaviour of coated or wrapped crystals is well reproduced by one exponential.

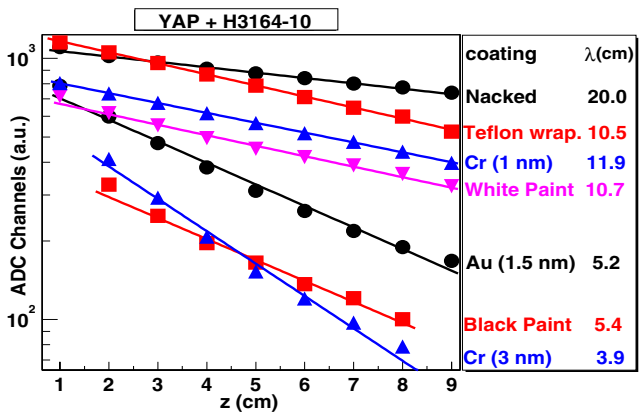

Fig. 7. Pulse height of the photopeak centroids as delivered by a H3164-10 Photomultiplier for 511 keV γ-rays impinging laterally on a 10 cm long YAP crystal at different z-positions. The different coatings of the crystal lateral surfaces are indicated in the right panel. The lines on the experimental points are exponential fits to the data. The resulting light attenuation lengths λ_{eff} are reported in the plot's legend. The extrapolation of the fits to z=0 gives a rough estimate of $N_0/2$ (see Eq. 1). The N_0 parameter is obviously also affected by the surface properties of the crystals.

The resulting light attenuation lengths λ_{eff} are reported in the right panel of Fig. 7. The investigated coatings result in λ_{eff} values in the range 3.9 to 11.9 cm, compared to 20.0 cm for the polished uncoated YAP crystal.

Although each of the coatings can effectively reduce λ_{eff}, only the Teflon wrapping is able to practically halve it and to maintain at the same time a high light yield. The metallic evaporation method has the advantage to allow tuning λ_{eff} to a desired value by changing the coating thickness.

The effectiveness of Teflon in reducing the photon attenuation length has also been proved for LYSO crystals. The effect of other coatings has not been tested on LYSO because currently only few crystal samples are available. Presumably the effects are the same as for YAP.

We remark that the extrapolations of the data in Fig.7 to z=0 (which correspond to $N_0/2$) show that the light collection efficiency is strongly dependant on the coating.

D. Reconstruction of the z-coordinate

The z-coordinate of the photon impact point is derived from the ratio of signals at the left and right bar ends using Eq. 1. Fig. 8 shows the mean value of the reconstructed z-coordinate for photo-peak events, plotted as a function of the true z-coordinate. These measurements result from averaging over many events, such that the statistical error of the mean value becomes negligible (smaller than the marker size in the figure). The left figure is for a polished uncoated YAP and the right one for a LYSO crystal. The data are very well described by a linear fit, proving the validity of the applied reconstruction method. A small deviation from linearity is observed towards the bar ends. Similar results have been obtained for coated and wrapped crystals. The non-linearity at the ends is slightly enhanced for the shorter λ_{eff} values.

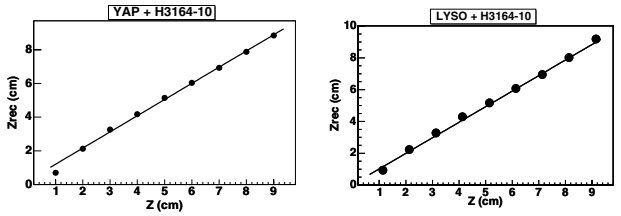

Fig. 8. The reconstructed scintillation positions (points) versus the effective ones for a polished YAP (left side) and LYSO (right side) crystal. The reconstruction is restricted to photopeak events. The continuous lines are linear fits to the data.

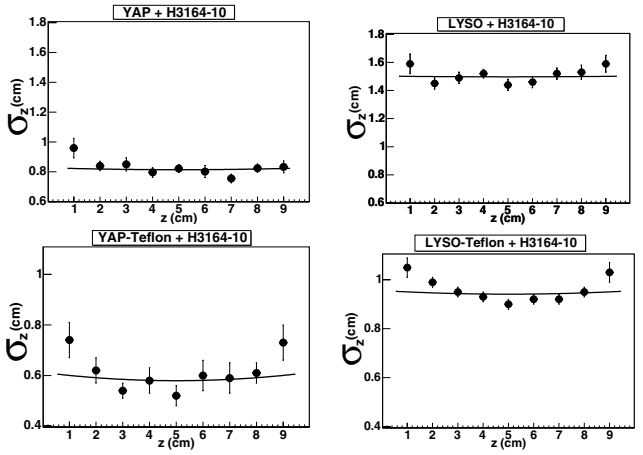

Fig. 9. The uncertainties in detecting a reconstructed scintillation point (standard deviations of the gaussians obtained in the reconstruction method) versus the effective z-position for YAP (left side) and LYSO (right side), polished (top panels) and Teflon wrapped crystals. Same abscissa scales in left and right panels, different in top and bottom panels.

The resolution in z-reconstruction for individual 511 keV photons is shown in Fig. 9, both for YAP and LYSO crystals, in polished and coated/wrapped condition. The upper two figures show the z-resolution for uncoated crystals. Values of σ_z = 0.8 and 1.45 cm are found for YAP and LYSO, respectively, essentially constant along the crystal length. The two lower plots show a significantly improved resolution when the crystals are wrapped with Teflon tape: σ_z = 0.6 and 1.0 cm. However the resolution degrades towards the ends of the crystals.

E. Precision of z-reconstruction and energy measurement

To achieve optimum performance both in energy and z-reconstruction resolution, the crystal has to provide both high light yield and an adequate short effective absorption length. These two requirements are to a certain extent contradictory and therefore a good compromise needs to be found.

The energy resolution σ_E/E has been derived from the photopeak of the sum spectra Q_R+Q_L, with a ^{22}Na source positioned at the centre of the crystal (z=5 cm). The two plots

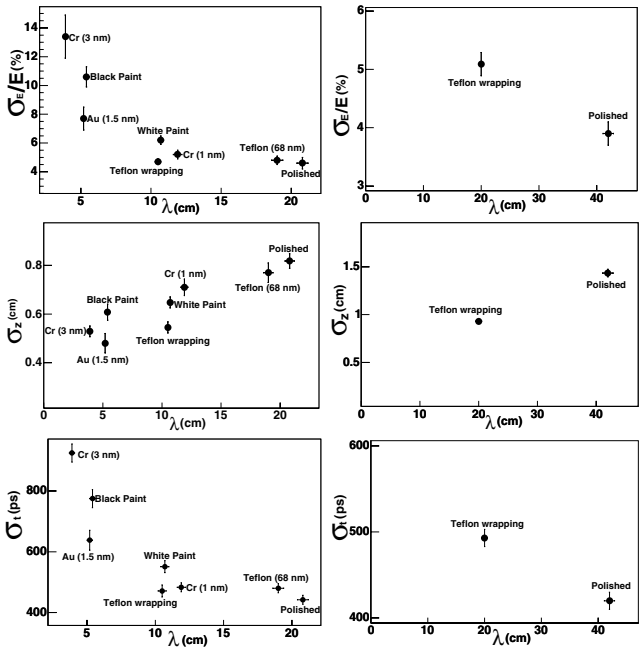

Fig. 10. The σ_E/E energy resolutions (top panels), the σ_z position resolutions (central panels), and the σ_t time resolutions (bottom panels) measured for scintillation in the crystal center (z=5 cm) for YAP (left side) and LYSO (right side) crystals at different λ_{eff} values.

in the upper part of Fig. 10 show the energy resolution of YAP and LYSO crystals as a function of the λ_{eff} values obtained with the different coatings/wrappings. As expected, the energy resolution degrades with decreasing λ_{eff}, while the z-resolution, measured at z=5 cm (see two central figures), shows the opposite behaviour: it improves with decreasing λ_{eff}. The resolution in the time difference of the left and right PMT signals, measured at z=5 cm, is displayed in the lower two plots. Its behaviour is similar to the one of the energy resolution.

The interpretation of these plots indicates that the Teflon wrapping represents the best compromise for 10 cm long YAP crystals. The experimental results are summarized in Table 1.

TABLE I

Achieved resolution with 10 cm long Teflon wrapped YAP and LYSO crystals at E_γ = 511 keV.

Scintillator	λ_{eff} (cm)	σ_z (cm)	σ_E/E (%)	σ_t (ps)
YAP+Teflon	10.5	0.55	5	500
LYSO+Teflon	20	0.9	5	500

To check the internal consistency of our measurements, we derive the number of photoelectrons from the measured energy resolutions. For this purpose the intrinsic resolution of the LYSO scintillator ($\sigma_E/E_{intr.}$ = 2% (LYSO) see [2] and references therein) is unfolded and the excess noise factor (ENF = 1.4) of the PMT is corrected for.

$$N_{pe} = \frac{ENF}{(\sigma_E / E)^2 - (\sigma_E / E)^2_{\text{intr.}}} \quad (3)$$

$$N_0 = N_{pe}(\tfrac{L_c}{2}) \cdot e^{\frac{L_c}{2}\lambda_{eff}} \quad (4)$$

The parameters N_0, listed in Table II, together with the measured values of λ_{eff}, allow us to calculate the expected resolution according to Eq. 1. We multiply the calculated σ_z values by a factor of 1.13 to account for path-length fluctuations [2] which are not included in Eq. 1. The obtained values together with the measured ones are also summarized in the table. We find good agreement on the level of 10%, except for 1nm Cr coating on YAP, where the difference is about 20%. The measured energy and spatial resolutions are consistent and proof the validity of our approach.

TABLE II

Comparison of expected and measured z-resolutions for YAP and LYSO crystals with different coatings at E_γ = 511 keV.

	λ_{eff} (cm)	σ_E/E (%)	N_o	σ_z (mm) expected	σ_z (mm) measured
YAP polished	20	4.7	814	9.0	8.2
YAP Tefl. wrap.	10.5	4.7	1021	4.7	5.4
YAP Cr (1nm)	11.9	5.5	852	5.7	7.0
YAP Cr (3nm)	3.9	13.3	285	4.9	5.3
LYSO polished	42	3.9	1407	13.4	15.0
LYSO Tefl. wrap.	20	5	817	8.9	9.0

III. CONCLUSIONS

In this paper YAP and LYSO scintillators have been characterized. The ratio of the N_0 values of YAP and LYSO (≈1.7) is in good agreement with the ratio of their light yields quoted in the literature (≈1.5). Excellent linearity in their energy response has been observed in the range 60 keV to 1.9 MeV. Scans along the crystal bars revealed a strictly exponential behaviour of the signal with the z-coordinate. This allows to reconstruct the z-coordinate form the ratio of the signals measured at the two bar ends. This last result proves an important aspect of the 3D Axial PET concept.

Both crystals were found to be significantly more transparent than reported in earlier works, particularly the polished LYSO crystals showed a very large effective optical absorption length of about 40 cm, i.e. a bulk value of about 50 cm. Wrapping or coating the crystal lateral surfaces allows to decrease the λ_{eff} value, but also influences N_o. The two parameters affect σ_z, σ_E/E and σ_t. Wrapped Teflon was found to be the best method to reduce λ_{eff} and σ_z while maintaining an acceptable N_0 value and hence also good σ_E/E and σ_t resolutions.

We foresee to realize the 3D Axial PET concept with custom designed HPDs, equipped with a thin sapphire entrance window, which leads to matched refractive indices. Simulations [2] predict a performance improvement in σ_z and σ_E/E. The metallic coatings will then be more suited to reach the necessary λ_{eff} values. Simulation calculations will be performed to extrapolate the presented results to other crystal lengths and to other scintillators. More importantly, experimental tests on $LaBr_3$ and LSO scintillators coupled to HPDs are under preparation.

REFERENCES

[1] The CIMA collaboration: http://www.cima-collaboration.org/.

[2] J. Seguinot et al., "Novel Geometrical Concept of High Performance Brain PET Scanner – Principle, Design and Performance Estimates", CERN PH-EP/2004-050.

[3] C. Joram, "Hybrid Photodiodes", Nucl. Phys. B (Proc. Supp.) 78 (1999) 407.

[4] A. Braem et al., "Novel design of a parallax free Compton enhanced PET scanner", NIM A 525 (2004) 268-274.

[5] Y. Shao et al., "Dual APD array readout of LSO crystals: optimization of crystal surface treatment", IEEE Trans.Nucl.Sci. 49 (2002) 649-654.

[6] P. Dorenbos, "Light output and energy resolution of Ce^{3+}-doped scintillators", NIM A 486 (2002) 208-213.

[7] D.J. Herbert, L.J. Meng, and D. Ramsden, "Investigating the Energy resolution of Arrays of Small Scintillation Crystals", IEEE Trans.Nucl.Sci. 49 (2002) 931-936.

[8] F.Vittori et al., "A study on light collection of small scintillating crystals", NIM A 452 (2000) 245.

[9] C. D'Ambrosio, H. Leutz, "Hybrid photon detectors", NIM A 501 (2003) 463-498.

[10] R. Perrino et al., "Timing measurements in long rods of BC408 scintillators with small cross-sectional area", NIM A 381(1996) 324-329.